The Journal of Experimental Biology 201, 385–401 (1998)
Printed in Great Britain © The Company of Biologists Limited 1998
JEB1172

THE CONTROL OF WING KINEMATICS AND FLIGHT FORCES IN FRUIT FLIES (*DROSOPHILA* SPP.)

FRITZ-OLAF LEHMANN* AND MICHAEL H. DICKINSON†

Department of Integrative Biology, University of California at Berkeley, Berkeley, CA 94720, USA

*Present address: Theodor-Boveri-Institut für Biowissenschaften, Lehrstuhl für Verhaltensphysiologie und Soziobiologie, Universität Würzburg Am Hubland, 97074 Würzburg, Germany

†Author for correspondence (e-mail: flymanmd@socrates.berkeley.edu)

Accepted 14 November 1997: published on WWW 14 January 1998

Summary

By simultaneously measuring flight forces and stroke kinematics in several species of fruit flies in the genus *Drosophila*, we have investigated the relationship between wing motion and aerodynamic force production. We induced tethered flies to vary their production of total flight force by presenting them with a vertically oscillating visual background within a closed-loop flight arena. In response to the visual motion, flies modulated their flight force by changing the translational velocity of their wings, which they accomplished *via* changes in both stroke amplitude and stroke frequency. Changes in wing velocity could not, however, account for all the modulation in flight force, indicating that the mean force coefficient of the wings also increases with increasing force production. The mean force coefficients were always greater than those expected under steady-state conditions under a variety of assumptions, verifying that force production in *Drosophila* spp. must involve non-steady-state mechanisms. The subtle changes in kinematics and force production within individual flight sequences demonstrate that flies possess a flexible control system for flight maneuvers in which they can independently control the stroke amplitude, stroke frequency and force coefficient of their wings.

By studying four different-sized species, we examined the effects of absolute body size on the production and control of aerodynamic forces. With decreasing body size, the mean angular wing velocity that is required to support the body weight increases. This change is due almost entirely to an increase in stroke frequency, whereas mean stroke amplitude was similar in all four species. Despite the elevated stroke frequency and angular wing velocity, the translational velocity of the wings in small flies decreases with the reduction in absolute wing length. To compensate for their small size, *D. nikananu* must use higher mean force coefficients than their larger relatives.

Key words: aerodynamics, locomotion, flight, scaling, *Drosophila* spp.

Introduction

In order to construct a satisfying explanation of insect flight, it is necessary to understand how their complex wing motion generates aerodynamic forces. In many studies over the past 15 years, researchers have determined that the range of lift coefficients insects must produce to support their body weight is typically greater than those that can be generated under steady-state conditions (for reviews, see Ellington, 1984*a*, 1995). This discrepancy has fueled a search for unsteady mechanisms by which wings generate circulation (Weis-Fogh, 1973; Maxworthy, 1979; Nachtigall, 1979; Ellington, 1995). Experiments on both two-dimensional (Dickinson and Götz, 1993) and three-dimensional (Maxworthy, 1979; Ellington *et al*. 1996) models have suggested that the process of delayed stall might be the primary mechanism by which insect wings achieve elevated aerodynamic performance. Recently, Wilmott *et al*. (1996) have succeeded in visualizing an attached vortex, the manifestation of delayed stall, on the flapping wings of a tethered hawkmoth (*Manduca sexta*). Although delayed stall, the 'clap and fling' and other yet-to-be-discovered mechanisms may explain how insects stay in the air, they cannot alone explain the aerodynamics of flight behavior. Many insects must perform elaborate aerial maneuvers in order to avoid predators, feed, secure territories and mate. Even in less-sophisticated forms of flight, animals must still modulate force production in order to take off, land and avoid collisions. Maneuverability involves the controlled modulation of aerodynamic forces, which insects can accomplish through changes in either the circulation produced by the wings or the velocity at which they translate. While insects control wing velocity by varying stroke frequency and amplitude, significant changes in circulation can result from more subtle alterations in stroke kinematics such as modifications in the angle of attack, wing camber or the speed of wing rotation.

The most direct means of identifying how insects modulate flight forces is to measure aerodynamic forces and stroke kinematics simultaneously during complex free-flight maneuvers. However, since it is difficult to measure flight forces

and subtle kinematic changes on freely flying insects, many previous studies have focused on hovering or near-hovering conditions during which flight forces and wing motion are constant from one stroke to the next (Weis-Fogh, 1973; Ellington, 1984*c*; Ennos, 1989). Nevertheless, several researchers have succeeded in quantifying the changes in wing kinematics associated with different flight speeds (dragonflies: Rudolph, 1976, Wakeling and Ellington, 1997; bees: Dudley and Ellington, 1990). Collectively, these studies find little or no correlation between stroke amplitude or frequency and forward velocity or total flight force. It may be premature, however, to assume that insects never use these kinematic changes to modify flight forces. Analyzed sequences in free-flight studies are typically short relative to the duration of many steering maneuvers and thus might provide only a sparse picture of the full behavioral repertoire. Detailed analyses of stroke kinematics over long periods are performed more easily on tethered animals (Nachtigall, 1966; Zanker, 1990; Lehmann, 1994), but such studies are suspect because it is difficult to determine whether the wing motion recorded under tethered conditions truly reflects those that the animal would produce in free flight. In particular, in tethered studies, it is possible that the insects do not produce enough force to sustain their own body weight. In order to circumvent these limitations, we have constructed an electronic flight arena in which closed-loop feedback enables the animal to control the motion of its visual world by actively changing its wing kinematics (Heisenberg and Wolf, 1984; Götz, 1987; Lehmann and Dickinson, 1997). By manipulating the visual feedback, we can make an animal modulate force production while simultaneously measuring stroke kinematics. By comparing the resulting force variation with the changes in stroke kinematics, we can investigate the means by which the animals actively modulate their aerodynamic output.

The aerodynamic performance of an airfoil is a function of its Reynolds number and, therefore, may potentially vary with body size. Although the effect of body size on wing performance should be minimal for most animals, the case may be different for small insects such as fruit flies that operate at Reynolds numbers ranging from 50 to 500. With decreasing body size, small insects face significantly larger viscous forces within the fluid that could attenuate circulatory mechanisms while simultaneously increasing the profile drag due to skin friction (Dickinson and Götz, 1993). This potential reduction in aerodynamic performance with decreasing body size compromises not only an animal's ability to stay in the air but also the facility with which it can steer. One difficulty with assessing the effects of scaling in aerodynamic performance is that changes in body size are often accompanied by changes in body shape. This problem may be partly circumvented by comparing closely related species of insects whose wings and body are morphologically similar over a large size range. Fruit flies within the genus *Drosophila* fit this criterion and are thus well suited for studying the effects of body size on wing kinematics and force production.

In the present study, we investigate the control and scaling of wing kinematics and force production in fruit flies of the genus *Drosophila*. For the first time, we provide accurate measurements of wing velocity and mean force coefficients over a wide range of different flight forces. We extended the analysis to flies of similar shape but with different body sizes to determine how aerodynamic performance changes with Reynolds number.

Materials and methods

Experimental setup

Data were collected from sixty-one 2- to 5-day-old female fruit flies. The animals were selected from laboratory colonies maintained at room temperature (22 °C) and reared on commercial *Drosophila* medium (Carolina Biological). We tested flies from four different species: *D. nikananu* Burly (N=11), *D. melanogaster* Meigen (N=27), *D. virilis* Sturtevant (N=10) and *D. mimica* Hardy (N=13), with body masses of 0.65±0.06 mg, 1.05±0.13 mg, 1.9±0.19 mg and 3.06±0.52 mg, respectively (means ± S.D.). Owing to variations in the egg content of the female flies, we deemed body length (measured from the front of the head capsule to the tip of the abdomen) to be a more reliable measure of body size than body mass.

We have previously provided a detailed description of the experimental apparatus (Lehmann and Dickinson, 1997), and give only a brief outline here. The flies were tethered rigidly between the head and notum and flown in a flight arena in which stroke amplitude, stroke frequency and total flight force were measured simultaneously under closed-loop conditions. An optically based transducer measured the component of total flight force parallel to the longitudinal body axis of the fly. Total flight force was estimated according to the measurements of Götz and Wandel (1984), who found that the total flight force vector in *D. melanogaster* was oriented at an angle of 24 ° with respect to the longitudinal body axis and did not vary with the animal's absolute orientation in space. By changing the relative stroke amplitude of its two wings, each fly controlled the angular (azimuth) velocity of a 30 ° wide vertical dark bar displayed in the arena. Under these conditions, the flies actively modulated their wing kinematics in order to stabilize the stripe in the front region of their visual field. While the fly actively controlled the vertical bar, we oscillated a superimposed pattern of diagonal stripes in the vertical direction. As the background pattern moved up and down, the fly modulated its total flight force in an attempt to stabilize the retinal slip. Since the four species differed somewhat in their response to the visual motion, we found it necessary to vary the stimulus parameters in order to evoke similar modulations in flight force. For *D. nikananu* and *D. mimica*, we occasionally replaced the sinusoidal variation in stripe velocity with square-wave variation, producing motion at a constant velocity that changed direction at regular intervals. To avoid cessation of flight by *D. nikananu* at low flight forces, we also varied the duty cycle so that the upward stimulus lasted longer than the downward stimulus.

After gluing the flies to their tether (Lehmann and Dickinson, 1997), we allowed them to cling to a small square piece of paper (cut from Kimwipe). Once aligned within the

chamber, we could elicit flight by providing a short air puff from below the fly, although some animals began to fly spontaneously and a few flies had already released their paper platform and started to fly by the time they were correctly positioned within the arena. In most cases, we recorded two flight sequences from each animal representing a mean flight time of 13±6 min (S.D.). During each experiment, we measured wingbeat frequency, left and right stroke amplitude, flight force, the angular position of the fixation stripe, and the vertical oscillation of the background pattern. All data channels were sampled continuously at 8.3 Hz using an AXOTAPE data acquisition system (Axon Instruments).

While measuring the kinematic variables and flight force, we also monitored the CO_2 efflux through the chamber. The energetic consequences of changes in body size and aerodynamic performance will be addressed in a forthcoming paper. Some of the kinematic and respirometry data from *D. melanogaster* presented here have been published previously in an analysis of muscle performance (Lehmann and Dickinson, 1997). For each fly, we calculated the mean values of all the data points within the flight recording that fell within the top 1 % (maximum) or bottom 1 % (minimum) of flight force or within 1 % of body weight (hovering).

Mean wing velocity and mean force coefficients

The mean total flight force, F_t, generated by the wing pair throughout the stroke may be estimated from a standard 'quasi-steady' formulation of flight force (Weis-Fogh, 1973; Ellington, 1984*e*):

$$F_t = \int_{r=0}^{R} \rho \overline{C_F} \overline{u_r^2}(r) c(r) \mathrm{d}r \,, \qquad (1)$$

where ρ is the density of the air (1.2 kg m^{-3}, Vogel, 1981), $\overline{C_F}$ is the mean force coefficient of the wing throughout the stroke, $\overline{u_r^2}(r)$ is the mean square relative velocity of each wing section, $c(r)$ is the chord length of the wing at a distance r from the base, and R is the total wing length. Because our methods cannot determine the instantaneous position of the wing, our analysis is based explicitly on the mean wing velocity throughout each stroke. The measurement of mean wing velocity depends on the waveform followed by the wing tip within the stroke plane (Ellington, 1984*c*). Since the wingbeat analyzer does not resolve the wing tip trajectory, we use a set of simple models that bracket the possible range of mean wing velocity values. The mean translational velocity of each wing section can be estimated from stroke amplitude, Φ, and stroke frequency, n, by:

$$\bar{u}(r) = \frac{1}{2} \left| \overline{\frac{\mathrm{d}\hat{\phi}}{\mathrm{d}\hat{t}}} \right| \Phi n r \,, \qquad (2)$$

using Ellington's (1984*c*) expression $\mathrm{d}\hat{\phi}/\mathrm{d}\hat{t}$ for dimensionless wing velocity. During motion, the wing experiences a relative velocity composed of the flapping velocity and the induced velocity of the wake. The ratio of mean translational velocity, $\bar{u}(r)$, to the mean relative velocity, $\overline{u_r}(r)$, is given by the relationship $\cos\beta/\cos\beta_r$, where β and β_r are the angles of the stroke plane and the relative stroke plane with respect to the net force vector (Ellington, 1984*e*). Substituting this expression for mean relative wing velocity into equations 1 and 2 yields:

$$F_t = \frac{1}{8} \rho \overline{C_F} \Phi^2 n^2 R^3 \bar{c} \left| \overline{\frac{\mathrm{d}\hat{\phi}}{\mathrm{d}\hat{t}}} \right|^2 \frac{\cos^2\beta}{\cos^2\beta_r} \int_{\hat{r}=0}^{\hat{r}=1} \hat{r}^2 \hat{c}(\hat{r}) \mathrm{d}\hat{r} \,, \qquad (3)$$

using the dimensionless forms of wing length and chord length, $\hat{r}$ and $\hat{c}$ (Ellington, 1984*b*) and $\bar{c}$ for the mean chord length. The integral in equation 3 is equal to the normalized second moment of wing area, $\hat{r}_2^2(S)$, which has a nearly constant value of 0.35 in the genus *Drosophila* (M. H. Dickinson, unpublished data). We estimated β_r by calculating the angular difference between the orientation of the stroke plane (Zanker, 1990) and the mean flight force vector in previous studies (David, 1978; Götz and Wehrhan, 1984; Lehmann, 1994; Dickinson and Götz, 1996). The results suggested that the stroke plane in hovering flies should be approximately horizontal, which we confirmed by examining free-flight sequences recorded using high-speed video. The orientation of the observed stroke plane (β=10–20 °) differs little from the calculated relative stroke plane, resulting in a mean value of $\overline{u_r^2}(r)$ that was only 3–4 % higher than $\overline{u^2}(r)$. Because this difference is not significant compared with expected measurement errors and other assumptions, we ignore the contribution of induced velocity to relative wing velocity and use equation 2 as a means of calculating $\overline{u_r}(r)$. Throughout the paper, we will use $\overline{u_r}(S)$ and $\overline{u_r^2}(S)$, the mean and mean square relative wing velocity at the center of area, for general comparisons of wing velocity. These values are calculated according to equation 2 with r=0.587R.

Incorporating $\hat{t}_f$ as the non-dimensional time in which the wing movement contributes to force production, we derive the mean force coefficient $\overline{C_F}$ from:

$$\overline{C_F} = \frac{8F_t}{\rho \Phi^2 n^2 R^3 \bar{c} (\overline{\mathrm{d}\hat{\phi}/\mathrm{d}\hat{t}})^2 \hat{t}_f \hat{r}_2^2(S)} \,, \qquad (4)$$

which is similar to equation 12 in Ellington (1984*e*). In the present analysis, we are deliberately lumping all circulatory mechanisms into a single term. A more detailed analysis would require defining both translational and rotational force coefficients. However, without instantaneous force records, flow visualizations and more detailed kinematics, it is difficult to untangle the relative contribution of multiple force-generating mechanisms. For this reason, we think it sensible to use a 'lumped' $\overline{C_F}$ for purposes of comparison. Obviously, any interpretation of $\overline{C_F}$ must take this simplification into account.

In most studies, lift is defined as the force component that acts in the opposite direction from gravity, while thrust is the force component in the horizontal plane. In hovering animals, thrust is zero and lift is equivalent to the total force vector. In *D. melanogaster*, the total flight force vector is oriented at an angle of approximately 24 ° with respect to the longitudinal body axis (Götz and Wandel, 1984). In addition, the mean stroke plane angle is constant with respect to the body axis. As

fruit flies maneuver, they tilt their whole body, as do helicopters, in order to orient the flight force vector (David, 1978).

Mean circulation and Reynolds number

The total mean circulation, $\overline{\Gamma}$, generated by the wings is proportional to the ratio of total flight force and mean wing velocity:

$$\overline{\Gamma} = \frac{F_t}{2\rho \overline{u}_r(S)R}, \quad (5)$$

We have arbitrarily defined $\overline{\Gamma}$ using the mean relative wing velocity at the center of area of the wing. As with our definition of $\overline{C_F}$, this expression for mean circulation lumps together both translational and rotational, steady and unsteady contributions to force production.

In a moving profile, the mean force coefficient depends on the Reynolds number. By convention (Weis-Fogh, 1973; Ellington, 1984*e*), we have calculated Reynolds number, *R*e, on the basis of the mean wing tip velocity $\overline{u_r}(R)$ as:

$$Re = \frac{\bar{c}\bar{u}_r(R)}{\nu}, \quad (6)$$

where ν is kinematic viscosity of air at 20 °C ($15\times10^{-6}\,m^2\,s^{-1}$; Vogel, 1981).

Results

Characteristics of flight initiation

In most cases, the flies began to fly while fixed within the flight arena, allowing us to quantify stroke kinematics and force production during the initial stages of flight. In all cases, the animals flew under closed-loop conditions from the onset of flight, but we did not begin vertical oscillation of the background pattern until 2 min after flight initiation. As shown in Fig. 1 for *D. melanogaster*, wingbeat frequency was high at the onset of flight, then decayed asymptotically towards a steady value within approximately 10 s. Stroke amplitude, in contrast, was low at the onset of flight but increased to a steady level within a similar time frame. This decrease in frequency and increase in amplitude was accompanied by a modest increase in flight force. In a few cases (indicated by the standard deviations in Fig. 1A), flies generated a large transient flight force during the first few seconds of flight.

In *D. melanogaster*, the earliest stages of voluntary and odor-induced flight initiations are kinematically distinct from those elicited by visual stimuli (Trimarchi and Schneiderman, 1995*a*) and appear to utilize different populations of descending interneurons (Trimarchi and Schneiderman, 1995*b*). To test whether there were any detectable differences in *voluntary* and *puff-initiated* flights within the arena, we compared the stroke amplitude, stroke frequency and flight

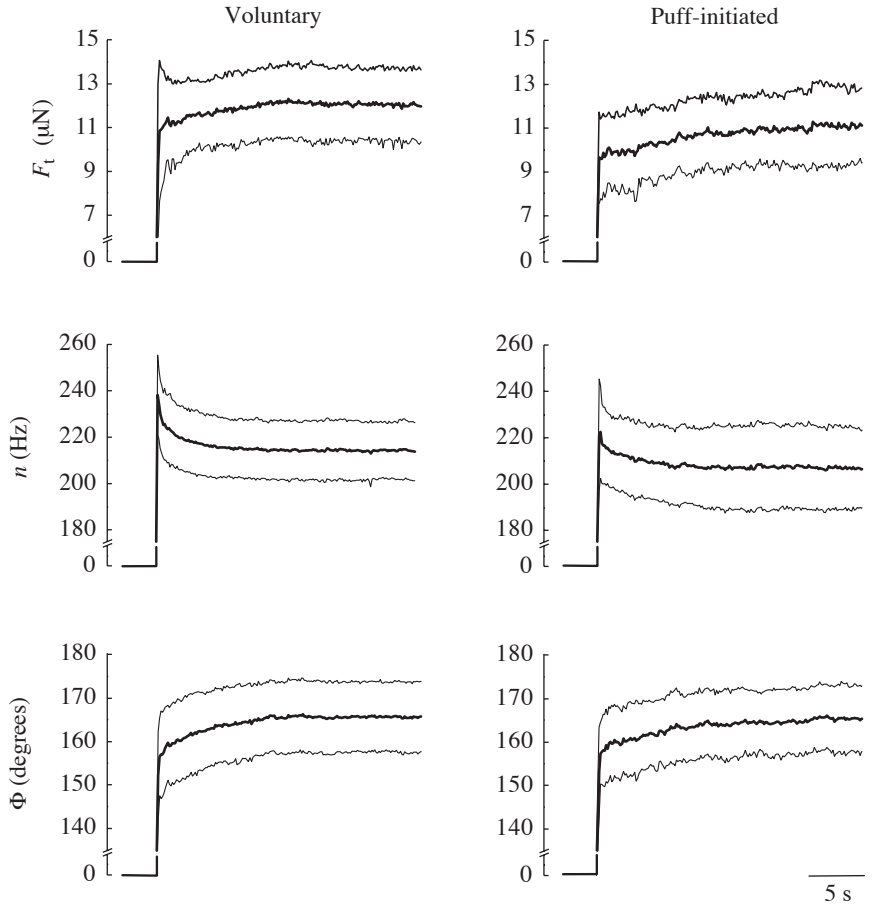

Fig. 1. Total flight force (F_t), stroke frequency (n) and stroke amplitude (Φ) during voluntary and puff-initiated take-off in tethered *Drosophila melanogaster*. The animals flew under closed-loop conditions from the onset of flight. The flies typically produced a high stroke frequency and low stroke amplitude during the first few seconds of flight. Over the next 10 s, stroke frequency declined and stroke amplitude increased to reach steady values. The thick line gives mean values from 47 voluntary (23 flies) and 19 puff-initiated (13 flies) flight starts; the thin lines represent ± S.D.

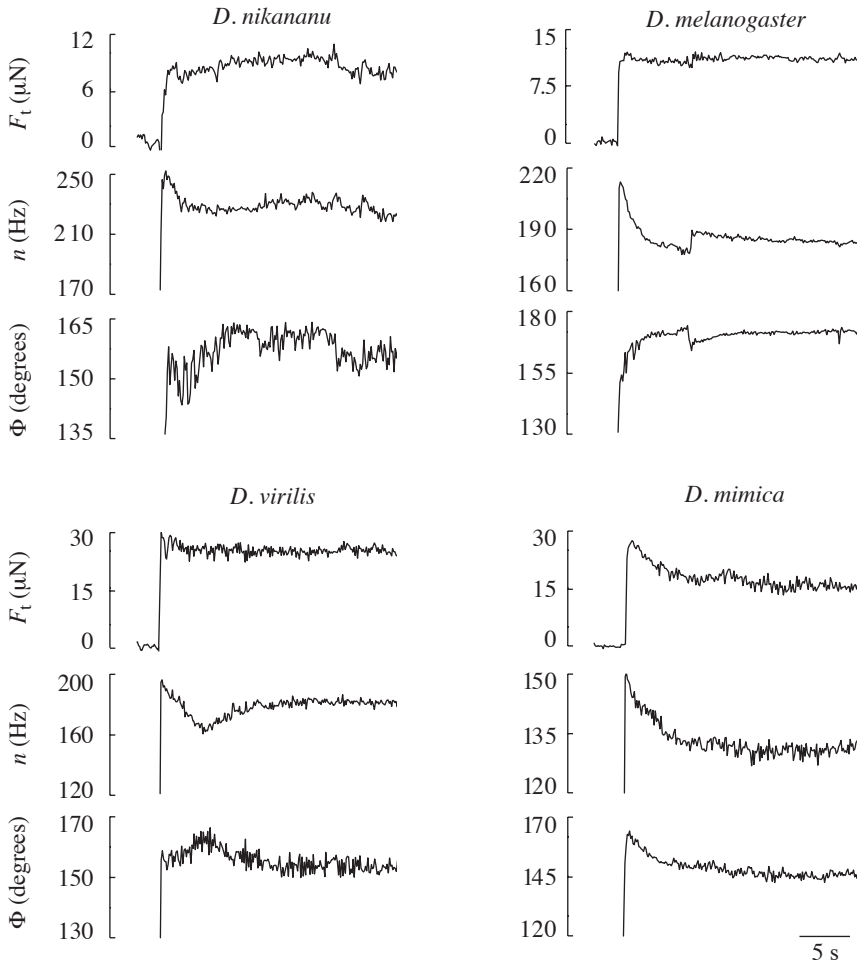

Fig. 2. Selected flight sequences from four species of fruit flies showing total flight force (F_t), stroke frequency (n) and stroke amplitude (Φ) at the onset of flight. The records indicate that flight initiation was not rigidly stereotyped. See text for details.

force following the two types of flight starts (Fig. 1). We did not detect any significant differences in either flight force or stroke kinematics following the two forms of flight initiation.

We observed the transient increase in stroke amplitude and decline in frequency following most of the flight starts in all four species. Averaged across the entire data set of 214 flight initiations, we measured a 6±4 % decrease in stroke frequency and a 3.3±4.7 % increase in stroke amplitude over the first 20 s of flight (mean ± S.D., 48 flies). Despite this general pattern, the behavior at the onset of a flight was by no means stereotyped (Fig. 2). For example, 6 s after starting to fly, the individual *D. melanogaster* shown in Fig. 2 made an abrupt transition in flight mode by rapidly increasing stroke frequency and reducing stroke amplitude. A similar alteration in kinematics is seen in the *D. virilis* individual shown in Fig. 2, although the transition from low frequency and high amplitude to high frequency and low amplitude was more gradual. Note that these kinematic transitions had little effect on the force trace, illustrating that flies are capable of producing the same flight force with different combinations of amplitude and frequency.

Kinematic relationships

While steering towards the vertical bar, the flies respond to up-and-down movement of the background pattern with a pronounced alteration in stroke kinematics and force production (Fig. 3). In an attempt to stabilize the oscillatory background movement, the flies varied the stroke amplitude of the wings by 21±8.3 ° (mean ± S.D., 61 flies, four species), amounting to a 14 % peak-to-peak modulation of the average amplitude (Table 1). In all four species, stroke amplitude reached a maximum at approximately 170 °, which probably reflects the morphological limit of the wing stroke. As reported previously for *D. melanogaster* (Lehmann and Dickinson, 1997), both stroke amplitude and frequency increased as flight force rose (Fig. 4; Table 2). At the highest flight forces, however, stroke frequency often decreased while stroke amplitude continued to rise. The transition occurred at flight forces roughly equal to the body weight of the fly.

As illustrated by the individual *D. mimica* shown in Fig. 3, some flies responded to the visual stimulus by producing short transient lift 'spikes' with magnitudes up to 65 % greater than the mean flight force. These events were correlated with transient increases in both stroke amplitude and frequency, and they are reminiscent of the torque spikes that flies generate in response to visual motion about the yaw axis (Heisenberg and Wolf, 1979, 1984). Since torque spikes are known to be correlated with unilateral occurrences of action potentials in

Table 1. *Peak-to-peak modulation of kinematic and aerodynamic measurements during vertical oscillation of the visual background pattern*

Species	N	$\Delta\Phi$ (%)	Δn (%)	$\Delta\overline{u_r}(S)$ (%)	$\Delta\overline{u_r^2}(S)$ (%)	$\Delta\overline{C_F}$ (%)	$\Delta\overline{\Gamma}$ (%)	$\Delta\overline{F_t}$ (%)	ΔRe (%)
D. nikananu	11	14±4.4	2.6±5.8	17±6.2	34±12	72±24	86±24	100±24	17±6.1
D. melanogaster	27	14±6.4	11±6.2	24±8.6	48±16	68±30	88±30	106±30	24±8.5
D. virilis	10	14±4.2	10±5.2	24±5.0	48±9.2	70±20	90±19	108±14	24±1.0
D. mimica	13	12±5.2	8.6±8.0	20±9.2	40±18	58±18	78±22	92±24	20±9.2

Φ, stroke amplitude; n, stroke frequency; $\overline{u_r}(S)$, mean relative wing velocity at the center of area; $\overline{C_F}$, mean force coefficient; $\overline{\Gamma}$, mean aerodynamic circulation; F_t, total flight force, Re, mean Reynolds number.

All values are expressed as mean ± S.D.

the second basalar (b2) muscle (Heide and Götz, 1996; Lehmann and Götz, 1996), it is possible that the lift spikes result from transient bilateral activation of b2.

Almost all the animals were capable of producing flight forces in excess of their body weight under tethered conditions: 91 % (10/11 flies) of *D. nikananu*, 96 % (26/27) of *D. melanogaster* and 100 % (10/10) of *D. virilis* (Table 3). Furthermore, approximately half of the animals were capable of generating flight forces of 140 % or more of their body weight (5/11, *D. nikananu*; 11/27, *D. melanogaster;* and 7/10, *D. virilis*). We have shown previously that in *D. melanogaster* these maximum tethered flight forces are at least 80 % of the maxima estimated from free-flight loading experiments (Lehmann and Dickinson, 1997). In contrast to the smaller

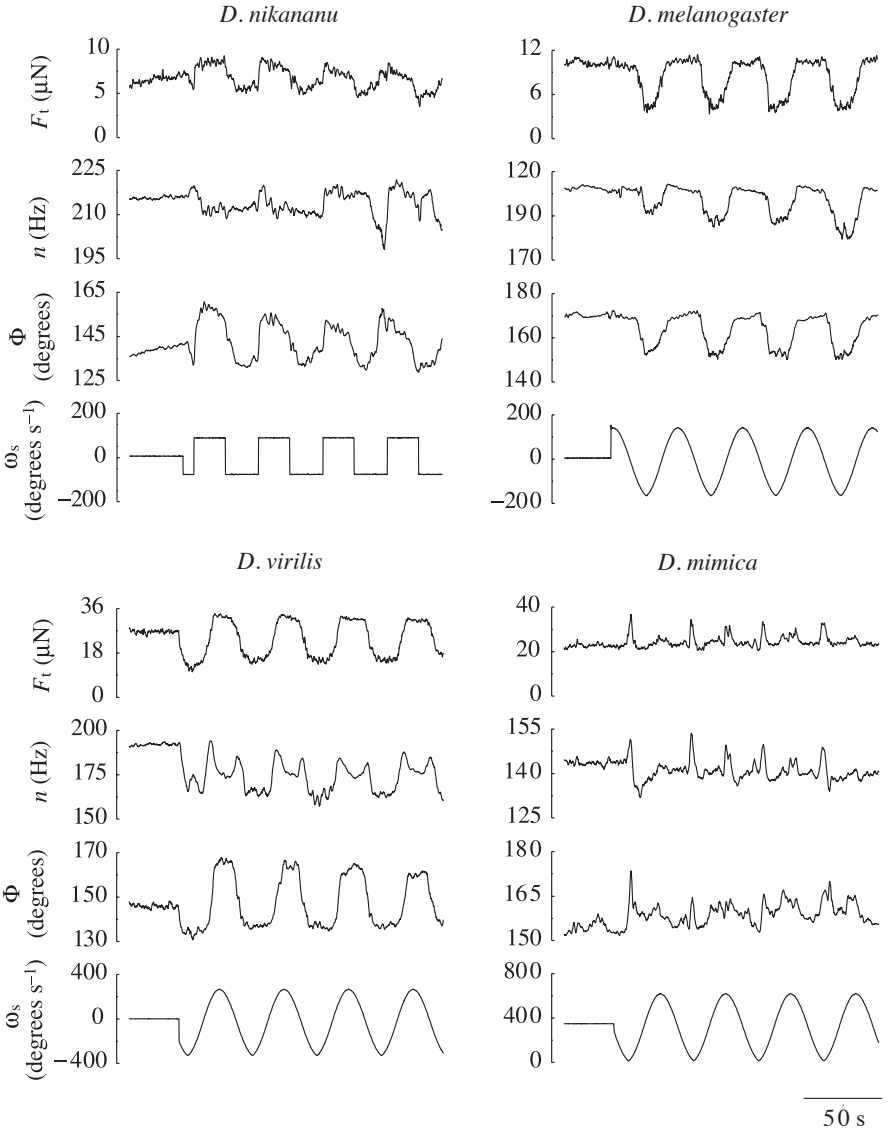

Fig. 3. Alterations of wing kinematics and flight force during vertical movement of the background pattern. In attempt to minimize the retinal slip, the flies modulated their total flight force (F_t) by approximately ±50 % in conjunction with simultaneous changes in stroke amplitude (Φ) and stroke frequency (n). As force production increased, stroke amplitude approached its morphological limit and stroke frequency typically began to decrease. This kinematic response is especially clear in the *Drosophila melanogaster* and *D. virilis* individuals shown here. Not all individuals exhibited such a stereotyped response, as illustrated by the *D. nikananu* flight sequence. In this case, the stroke amplitude of the fly tracked the visual pattern closely, but the changes in stroke frequency were more erratic. As illustrated by the *D. mimica* example, flies occasionally responded to pattern motion by generating lift spikes correlated with transient increases in stroke amplitude and stroke frequency. The bottom trace shows the angular velocity of the background stripes (ω_s). A positive value of ω_s indicates that the chevron pattern moves upwards.

Table 2. *Correlation coefficients (r^2) between kinematic and aerodynamic variables*

Species	*N*	Φ *versus* F_t	*n versus* F_t	$\overline{u_r}$ *versus* F_t	$\overline{u_r^2}(S)$ *versus* F_t
D. nikananu	11	0.48±0.21	0.20±0.17	0.52±0.19	0.52±0.19
D. melanogaster	27	0.70±0.23	0.40±0.22	0.76±0.17	0.76±0.17
D. virilis	10	0.68±0.13	0.33±0.14	0.76±0.08	0.76±0.09
D. mimica	13	0.63±0.13	0.13±0.15	0.48±0.21	0.48±0.21

Abbreviations are as in Table 1.
All regressions are significant ($P<0.001$).
Values are means ± S.D.

species, *D. mimica* exhibited the weakest flight performance within the flight arena. Only 23 % (3/13) of these flies generated flight forces exceeding their body weight, and the highest force produced by any *D. mimica* individual was only 120 % of body weight. We have rarely seen individuals of this Hawaiian species hover within their culture containers or upon release within the laboratory, suggesting that it may not be as adept at flight at a low advance ratio as are smaller drosophilids.

Aerodynamic relationships

In all flies, total flight force was correlated with both the mean relative wing velocity and the mean square relative wing velocity (Table 2, $P<0.001$, two-tailed *t*-test, 61 flies). However, changes in velocity cannot explain all of the variations in total flight force. As shown in Fig. 5, the flies responded to vertical motion of the background pattern with a coordinated modulation of both the mean relative velocity, $\overline{u_r}(S)$, and the mean force coefficient, $\overline{C_F}$. In Fig. 6 we have plotted the instantaneous flight force against both the mean square relative velocity, $\overline{u_r^2}(S)$, and $\overline{C_F}$ for the flight sequences shown in Fig. 5. In all four species, $\overline{C_F}$ is lowest at minimum flight force and approximately doubles at peak force levels (Table 3). Although this large change in $\overline{C_F}$ is probably due to the fly's active modulation of wing kinematics, there are two alternative explanations. First, the apparent rise in $\overline{C_F}$ might reflect no more than an underestimate of mean wing velocity caused by a change in the gross pattern of the wing stroke. For example, although we assume in this particular calculation (but see Table 4) that the wing tip follows a sawtooth trajectory with respect to time, the flies might switch from a sinusoidal pattern at low force production to a sawtooth pattern when generating large forces. However, such alterations could account for no more than 30 % of the twofold change in $\overline{C_F}$. Second, it is possible that the increase in aerodynamic performance is a passive result of the change in Reynolds number that occurs as stroke velocity increases. Fig. 7 plots $\overline{C_F}$ as a function of mean relative wing velocity and Reynolds number for a typical flight sequence in *D. melanogaster*. The instantaneous Reynolds number does vary significantly ($P<0.001$) from a value of approximately 115 at low force production to 175 during the generation of peak forces. However, even within the domain of intermediate Reynolds numbers, this small change in *Re* is unlikely to explain a doubling of $\overline{C_F}$ (Dickinson and Götz, 1993). It seems more likely that the changes in $\overline{C_F}$ represent an active modulation of stroke kinematics to increase the wing's aerodynamic performance.

Table 3. *Kinematic and aerodynamic measurements in four drosophilid species*

Species	*N*	Performance	Φ (degrees)	*n* (Hz)	$\overline{u_r}(S)$ ($m\,s^{-1}$)	$\overline{u_r^2}(S)$ ($m^2\,s^{-2}$)	$\overline{C_F}$	$\overline{\Gamma}\times10^3$ ($m^2\,s^{-1}$)	F_t (μN)	*Re*	F_t/w_b
D. nikananu	11	Minimum	142±5	213±18	1.20±0.11	1.44±0.28	1.35±0.36	0.54±0.18	3.1±1.2	90±10	0.48±0.19
D. nikananu	10	Hovering	153±5	222±16	1.34±0.10	1.81±0.26	2.30±0.32	1.02±0.08	6.3±0.6	101±9	1
D. nikananu	11	Maximum	164±5	218±16	1.42±0.13	2.02±0.38	2.86±0.42	1.33±0.19	8.8±1.7	107±12	1.4±0.28
D. melanogaster	27	Minimum	148±9	190±18	1.38±0.14	1.92±0.39	0.97±0.40	0.55±0.23	4.4±2.0	129±14	0.44±0.23
D. melanogaster	26	Hovering	162±8	209±15	1.66±0.14	2.78±0.45	1.59±0.20	1.07±0.09	10.3±1.2	154±14	1
D. melanogaster	27	Maximum	169±7	212±12	1.76±0.14	3.12±0.47	1.88±0.29	1.34±0.13	13.6±1.5	163±15	1.34±0.20
D. virilis	10	Minimum	137±5	158±11	1.51±0.17	2.32±0.48	0.85±0.37	0.72±0.32	8.5±2.4	194±12	0.46±0.13
D. virilis	10	Hovering	144±6	171±11	1.72±0.21	2.99±0.65	1.43±0.43	1.38±0.40	18.7±1.9	219±14	1
D. virilis	10	Maximum	158±6	175±9	1.93±0.20	3.75±0.71	1.73±0.57	1.88±0.67	28.7±5.5	247±14	1.54±0.31
D. mimica	13	Minimum	145±8	133±10	1.51±0.15	2.29±0.47	0.85±0.27	0.71±0.27	10.0±4.5	189±26	0.33±0.13
D. mimica	3	Hovering	162±1	146±1	1.87±0.08	3.49±0.29	1.77±0.30	1.84±0.25	31.9±5.0	238±21	1
D. mimica	13	Maximum	163±3	145±10	1.84±0.15	3.42±0.56	1.50±0.32	1.51±0.34	25.6±6.8	230±23	0.87±0.18

For each fly, we calculated the mean values of all data points within the flight sequence sorted according to three non-overlapping ranges of flight force: top 1% (maximum), bottom 1% (minimum) and within 1% of body weight (hovering).
Abbreviations are as in Table 1; w_b, body weight.
Values are means ± S.D.

Table 4. *Mean force coefficients calculated for different stroke trajectories when flight force was equal to body weight*

	N	50% up 50% down	50% up 50% down	30% up 70% down	50% up 50% down	50% up 50% down	30% up 70% down
$\overline{\lvert d\hat{\phi}/d\hat{t}\rvert^2}\hat{t}_f$		16	8	5.7	19.7	9.9	7.1
D. nikananu	10	2.3±0.3	4.6±0.6	6.4±0.9	1.9±0.3	3.7±0.5	5.2±0.7
D. melanogaster	26	1.6±0.2	3.2±0.4	4.4±0.6	1.3±0.2	2.6±0.3	3.6±0.5
D. virilis	10	1.4±0.4	2.9±0.9	4.0±1.2	1.2±0.2	2.3±0.7	3.2±1.0
D. mimica	3	1.8±0.3	3.5±0.6	5.0±0.8	1.4±0.3	2.9±0.5	4.0±0.7

Stroke symmetry is indicated by the percentages for each half-stroke.
The involvement of strokes in force production is indicated by the thickness of shading.
Values are means ± S.D.
$\hat{t}_f$, dimensionless stroke time contributing to weight support; $\overline{\lvert d\hat{\phi}/d\hat{t}\rvert^2}$ mean square of dimensionless wing velocity.

The above results suggest that flies are capable of modulating flight force by changing both relative wing velocity and the mean force coefficient. Close examination of individual flight sequences indicates that flies can control these two parameters independently. The four flight sequences shown in Fig. 8 provide examples of (i) a decrease in $\overline{C_F}$ while wing relative velocity increases (Fig. 8A), (ii) different values of $\overline{C_F}$ produced at the same relative wing velocity (Fig. 8B), (iii) rectification of $\overline{C_F}$ at high relative wing velocity (Fig. 8C), and (iv) an increase in $\overline{C_F}$ while relative wing velocity decreases (Fig. 8D). We found evidence for decoupling between stroke velocity and force coefficient modulation in all four species.

The magnitude of the mean force coefficients

The precise magnitude of the mean force coefficient is dependent on the trajectory of the wing stroke and whether or not both strokes are involved in force generation. Kinematic studies in *D. melanogaster* indicate that the motion of the wing in the stroke plane is more accurately characterized as a sawtooth than as a simple harmonic and that the downstroke represents 65 % of the stroke cycle (Zanker, 1990; Lehmann, 1994). Evidence as to whether both strokes are involved in force production is contradictory, since flow visualizations suggest that little or no vorticity is generated during the upstroke, whereas instantaneous force measurements suggest that some force production occurs during both strokes (Dickinson and Götz, 1996). Because of these uncertainties, we have calculated $\overline{C_F}$ using a number of different assumptions that should encompass the range of actual values. This was carried out by changing the $\overline{\lvert d\hat{\phi}/d\hat{t}\rvert^2}\hat{t}_f$ terms in equation 4. Table 4 presents these estimates for all four species under conditions in which the total mean flight force, F_t, was equal to body weight. The most conservative (but unrealistic) model is one in which the wing motion is described by a pure sine wave with both half-strokes contributing equally to force generation. Under these conditions, $\overline{C_F}$ estimates vary from 1.2 in *D. virilis* to 1.9 in *D. nikananu*. Even in this conservative model, the $\overline{C_F}$ values are higher than steady-state measures of translational lift force coefficients on real and model fly wings (Vogel, 1967*a*; Nachtigall, 1985; Dickinson and Götz, 1993). These estimates are, however, comparable to steady-state values of the total force coefficient, the trigonometric resultant

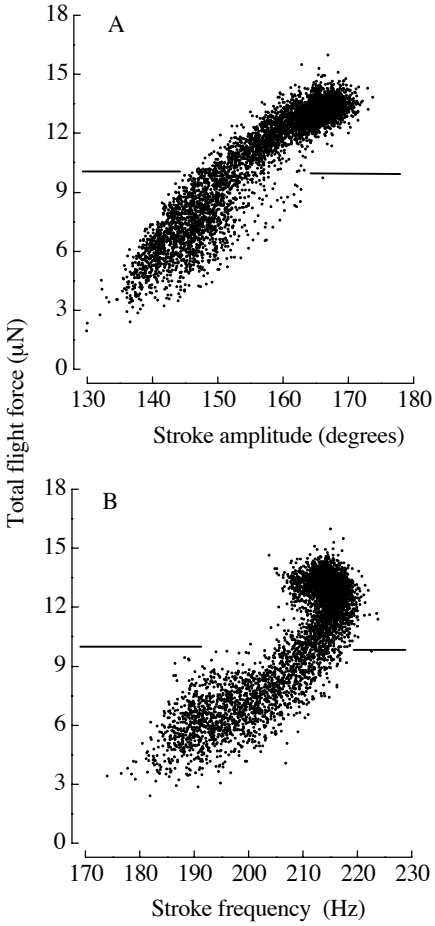

Fig. 4. Relationship between wing kinematics and total flight force for a single *Drosophila melanogaster*. (A) Stroke amplitude increases monotonically with total flight force. The slope of this relationship decreases at flight forces in excess of the animal's weight. (B) Stroke frequency first increases and then decreases with increasing flight force. The solid line indicates the fly's body mass of 1.0 mg. Data in each graph were sampled during a 11 min flight sequence (*N*=5572).

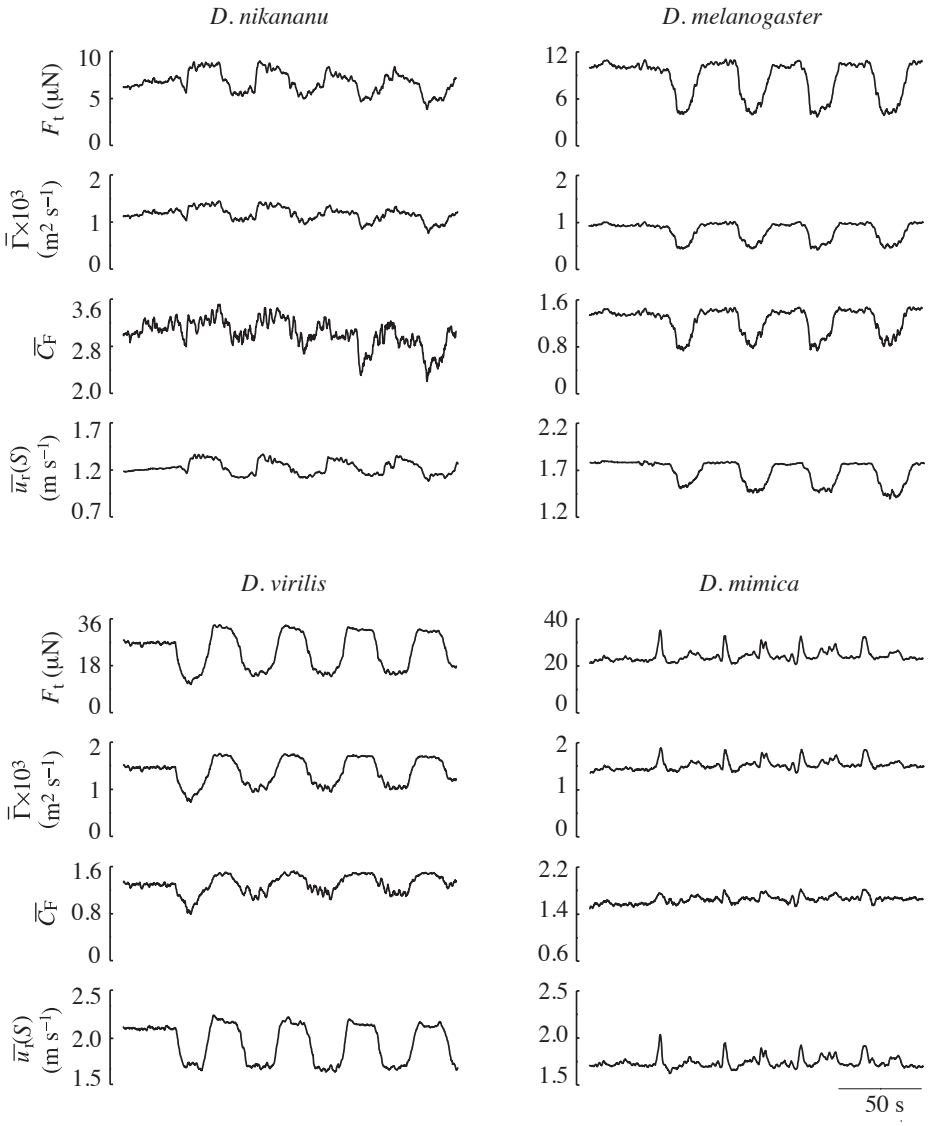

Fig. 5. Flight sequences from four species showing coordinated modulation of mean relative wing velocity of the center of area, $\overline{u_r}(S)$, mean circulation, $\bar{\Gamma}$, and mean force coefficient, $\overline{C_F}$ during changes in flight force, F_t. The data correspond to the sequences shown in Fig. 3. The values were calculated under the assumption that the wing tip followed a symmetrical sawtooth with both strokes contributing to weight support (see Table 4).

of the lift and drag coefficients (Dickinson, 1996; and see below). The most liberal model assumes that the wing follows an asymmetrical triangular waveform and that only the downstroke contributes to force generation. Under these assumptions, $\overline{C_F}$ ranges from 4.0 in *D. virilis* to 6.4 in *D. nikananu*.

Scaling of wing kinematics and aerodynamic force generation

Among the four species examined, the stroke amplitude measured when the flight force was equal to body weight did not change significantly with body size (r^2=0.07, P=0.11, 49 flies; Fig. 9A). All flies support their body weight at a mean stroke amplitude of approximately 160°, with the exception of *D. virilis*, which tended to fly with a stroke amplitude approximately 20° lower than in the other species. With increasing body size, stroke frequency decreased from approximately 250 Hz in the smallest flies to 150 Hz in the largest (r^2=0.61, P<0.001, Fig. 9B). This reduction in frequency resulted in a decrease in the angular velocity of the wings of larger flies (r^2=0.60, P<0.001, Fig. 9C). However, since wing length increased nearly isometrically with body size, the translational velocity of the wing was actually greater in larger flies, increasing from approximately 1.2 m s^{-1} in *D. nikananu* to 2.0 m s^{-1} in *D. mimica* (r^2=0.55, P<0.001, Fig. 9D). Because the increase in stroke frequency was steep enough to maintain a constant translational velocity of the wing, the smallest flies must produce a higher mean force coefficient in order to stay in the air (r^2=0.32, P<0.001, Fig. 9E). The averaged $\overline{C_F}$ of *D. nikananu* was significantly greater (P<0.001, two-tailed t-test) than the values for *D. melanogaster*, *D. virilis* and *D. mimica*. The mean force coefficients among the three larger species did not differ significantly from one another. Across all four species, there was a significant decrease in maximum flight force with increasing body length (r^2=0.13, P<0.05, Fig. 9F). However, this trend only reflected the lower performance of the largest species, *D. mimica*, within the arena. There was no significant difference in maximum flight force among *D. melanogaster*,

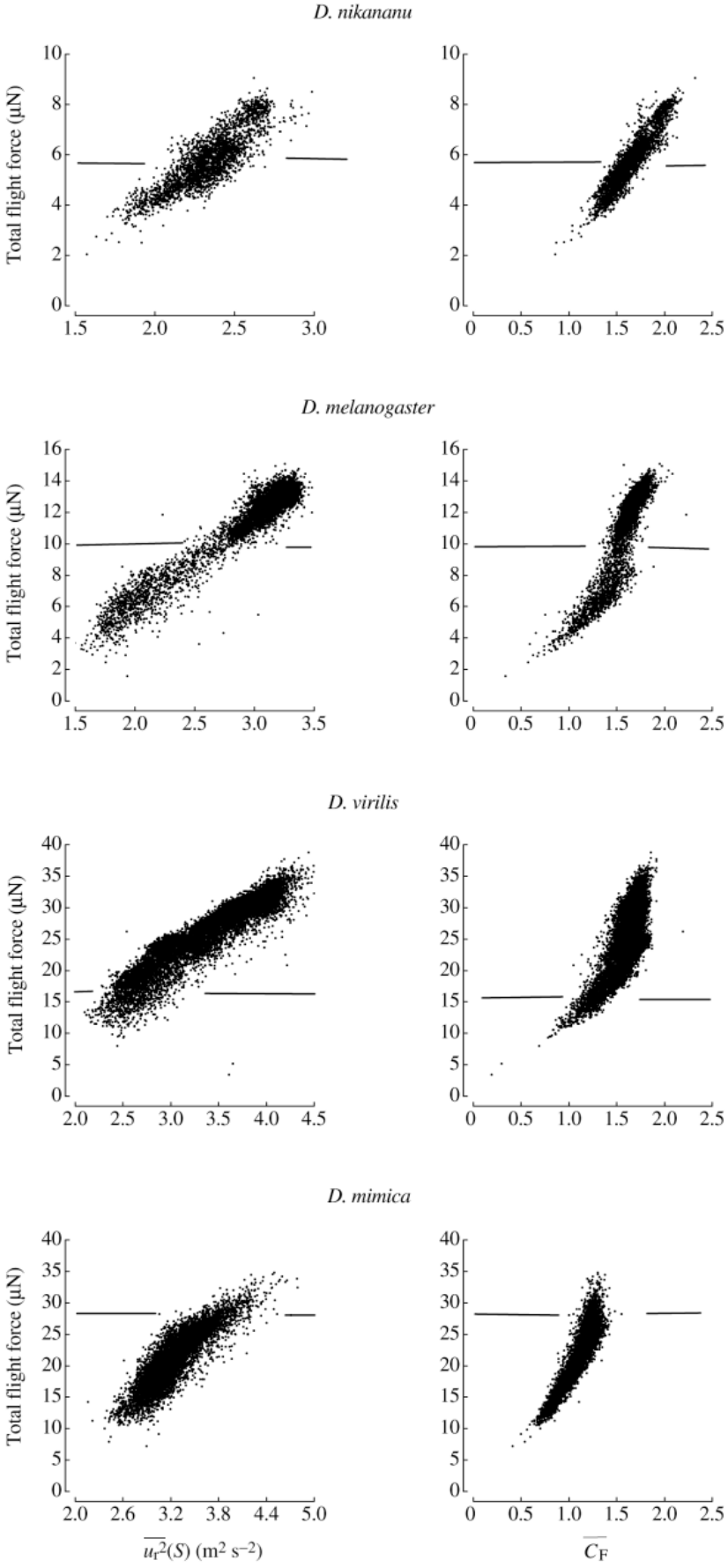

Fig. 6. Flight forces correlate with both the mean square of relative wing velocity of the center of area, $\overline{u_r^2}(S)$, and mean force coefficient, $\overline{C_F}$, in all four drosophilid species. In order to double total flight force, fruit flies increase $\overline{u_r^2}(S)$ by approximately 50 %, and increase $\overline{C_F}$ by approximately 70 %. The data were collected from two flight sequences for each fly lasting 13±6 min each (N=6453±3179, mean ± S.D.). The solid line in each panel indicates the fly's body weight.

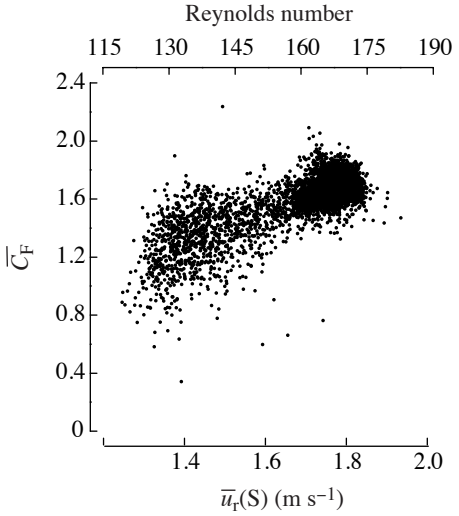

Fig. 7. Mean force coefficient, $\overline{C_F}$, *versus* instantaneous Reynolds number and mean relative wing velocity of the center of area, $\overline{u_r}(S)$. The small change in Reynolds number is unlikely to explain the doubling of the force coefficient. The fly supports its body weight at a Reynolds number of approximately 160. Data recorded during a 12 min flight by a single *Drosophila melanogaster* (N=5949).

D. virilis and *D. mimica*, whereas the values for all three of these smaller species were significantly higher than in *D. mimica* (P<0.001, two-tailed t-test).

One possible explanation for the elevated values of in *D. nikananu* is that this species operates at a higher Reynolds number. However, the mean Reynolds number increased linearly with body size across all four species examined (r^2=0.91, P<0.001, Fig. 10A). Thus, in conflict with the expectations of steady-state aerodynamic theory (Schlichting, 1979), we found a significant negative correlation between Reynolds number and $\overline{C_F}$ (r^2=0.53, P<0.001, Fig. 10B).

Discussion

These flight arena experiments have provided new insights into how different species of fruit flies generate and control the production of aerodynamic forces. We have shown that tethered fruit flies can modulate flight forces between 50 and 150 % of their body weight in response to vertical oscillation of a visual background (Table 2). As expected from even simple aerodynamic models, total flight force was correlated strongly with the translational velocity of the wings, which the flies altered by modulating both the frequency and amplitude of the stroke. Not all of the variation in flight force could be explained by changes in wing velocity, indicating that flies also control force production by modulating the mean force coefficient of their wings (Figs 5, 6). The values of $\overline{C_F}$ measured when the flight force was equal to body weight were always greater than 1, corroborating earlier studies which indicate that force production in *Drosophila* spp. involves non-steady aerodynamic mechanisms (Ennos, 1989; Zanker and Götz, 1990; Dickinson, 1996). As shown in Fig. 8, fruit flies

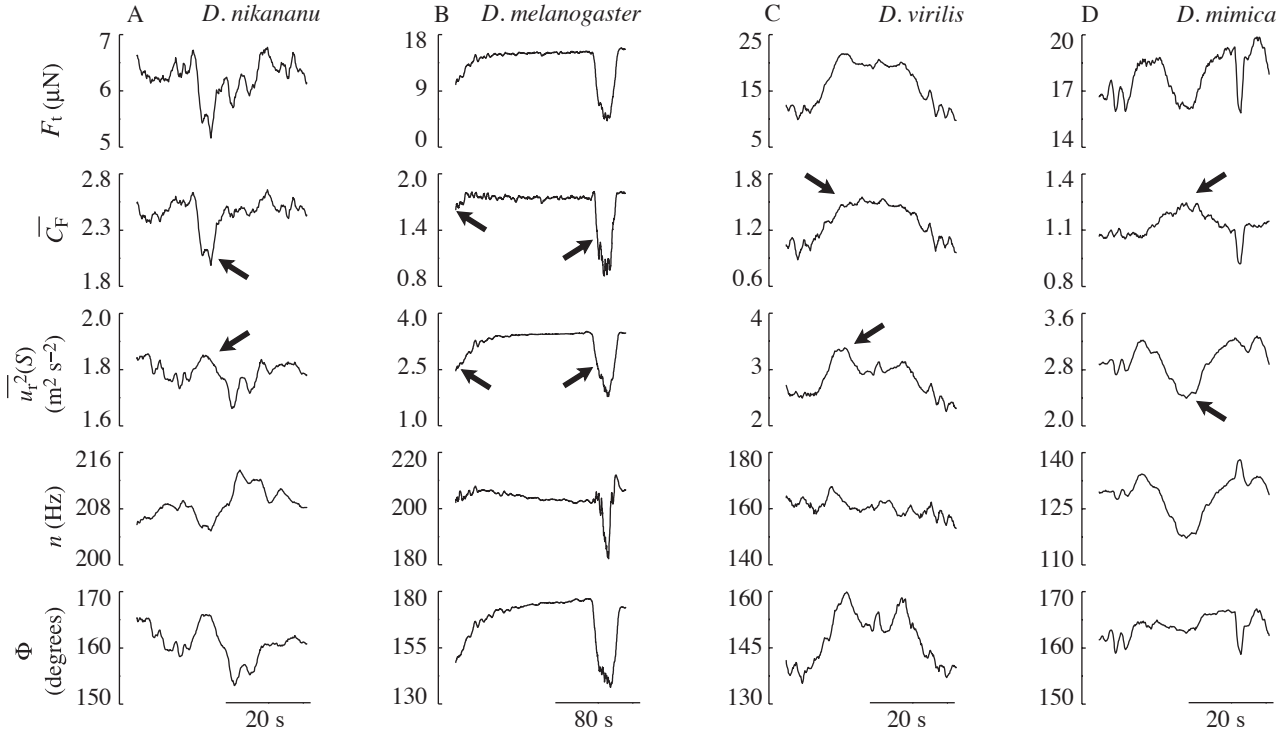

Fig. 8. Examples of flight sequences from four drosophilid species. During modulation of total flight force, F_t, mean square relative wing velocity of the center of area, $\overline{u_r^2}(S)$, and mean force coefficient, $\overline{C_F}$, can be controlled independently (arrows). Changes in wing velocity are accomplished through modulation of both stroke frequency, n, and stroke amplitude. Φ. See text for further details.

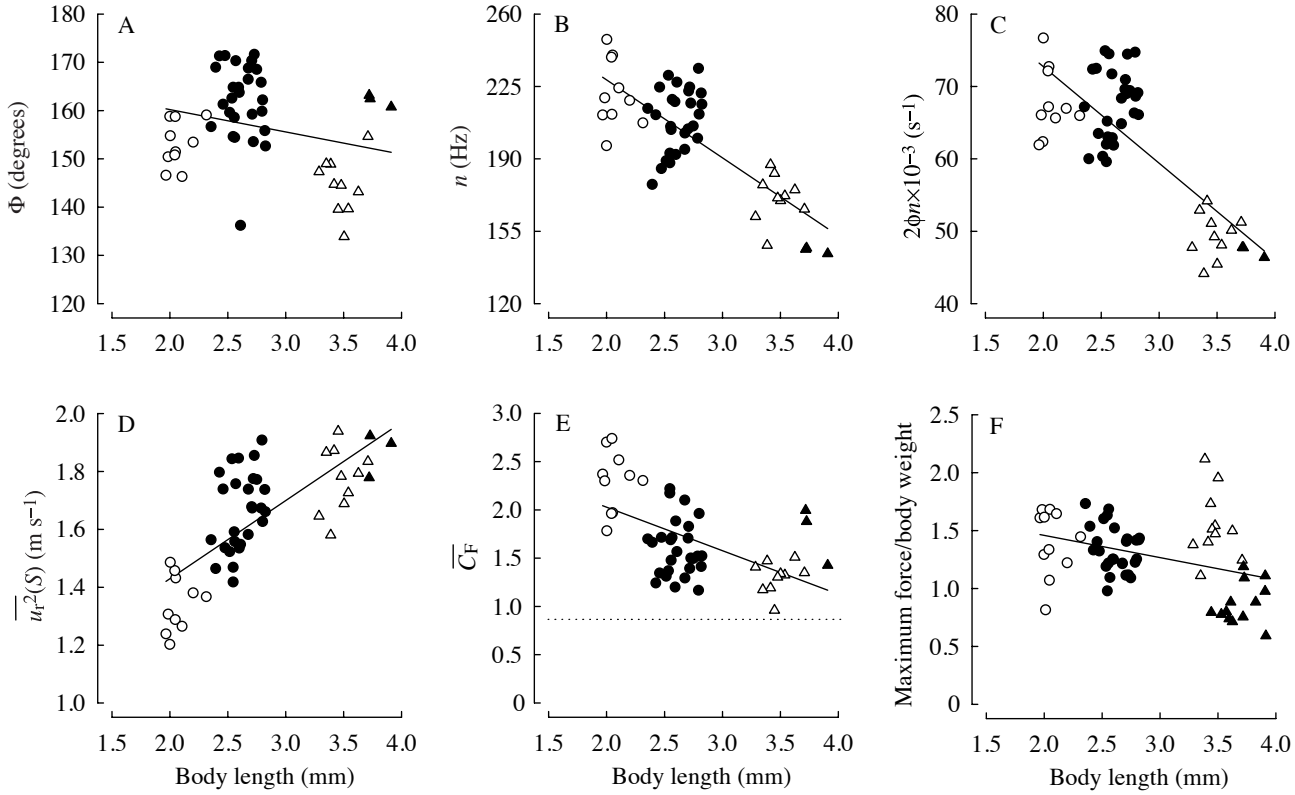

Fig. 9. The scaling of wing kinematics and aerodynamic force production in four drosophilid species. Each symbol represents the mean value of all points collected when a fly produced a flight force that was equal to its body weight ±1 %. Calculations were based on the symmetrical sawtooth velocity model with both half-strokes contributing equally to weight support (see Table 4). The dotted line in E indicates the maximum steady-state lift coefficient of *Drosophila virilis* wings (Vogel, 1967). Open circles, *D. nikananu* (N=10); filled circles, *D. melanogaster* (N=26); open triangles, *D. virilis* (N=10); filled triangles, *D. mimica* (A–E, N=3; F, N=11). Regression equations (A) y=169–4.64x, r^2=0.067, P=0.11; (B) y=303–37.6x, r^2=0.61, P<0.0001; (C) y=99.4–13.3x, r^2=0.060, P<0.001; (D) y=0.891+0.270x, r^2=0.55, P<0.001; (E) y=2.93–0.451x, r^2=0.32, P<0.001; (F) y=1.84–0.192x, r^2=0.13, P<0.05; Abbreviations are as in Table 1; 2ϕn, angular velocity of the wing.

are capable of controlling wing velocity and the mean force coefficient independently, suggesting that the underlying neuromuscular control of these two parameters is functionally distinct to some degree.

Comparative studies on the four species of *Drosophila* indicate that the mean angular velocity of the wings increases with decreasing body size (Fig. 9C). This increase is explained almost entirely by a size-dependent change in stroke frequency. However, the increase in stroke frequency in small flies is not enough to compensate for the reduction in translational velocity that occurs as the absolute length of the wing decreases (Fig. 9D). In order to support their body weight, the smallest species that we examined, *D. nikananu*, must generate mean force coefficients that are approximately 1.5 times those produced by larger congeneric species.

Force production under closed-loop conditions

The modulation in total flight force (Table 1) that we measured was much larger than found that in a previous study using a vertical motion stimulus (Götz, 1983). In the earlier study, the vertical open-loop stimulus was not combined with closed-loop control of a horizontally moving target. Active optomotor feedback of motion in the horizontal direction apparently renders the fly more sensitive to a vertically oscillating visual stimulus. This feedback-dependent sensitivity of the flight control system is reminiscent of the enhanced response of flies to a rotational bias under closed-loop conditions compared with their response to an identical visual stimulus under open-loop conditions (Heisenberg and Wolf, 1988). Even in the absence of the vertical stimulus, most flies in the present study (with the exception of *D. mimica*) generated forces that were near or even exceeded those required to support body weight, so long as they were engaged in closed-loop control of a vertical stripe. These observations, together with those of Heisenberg and Wolf (1988), suggest that active control of the visual world around the yaw axis is an essential feature of flight behavior that may gate the fly's response to other stimuli. The greatest artifact introduced by simple tethering may not be the lack of motion *per se*, but rather the absence of active optomotor feedback.

The neuromuscular control of wing velocity

Drosophilid flies vary flight force in part by modulating the translational velocity of their wings, which they control

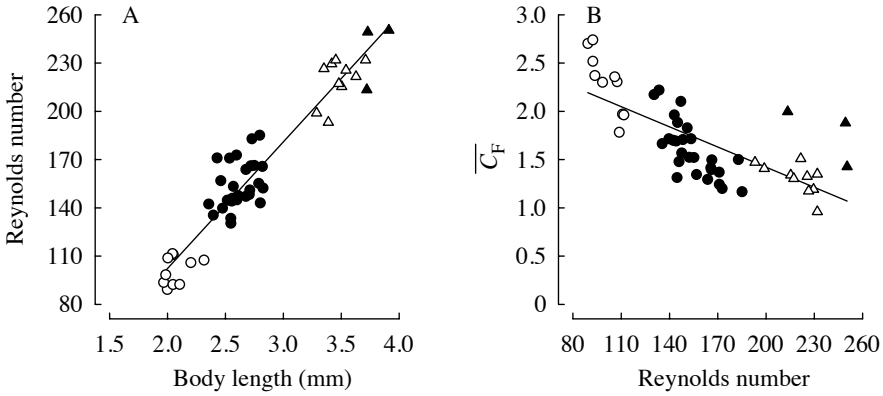

Fig. 10. (A) Reynolds number *versus* body length for four drosophilid species. Reynolds numbers were calculated using the wing-tip velocity when the animals were producing a flight force equal to their body weight. (B) Scaling of the mean force coefficient as a function of Reynolds number. Regression equations (A) $y=-54.8+78.7x$, $r^2=0.91$, $P<0.001$; (B) $y=2.81-6.97x$, $r^2=0.53$, $P<0.001$. Symbols and *N* are as in Fig. 9

through changes in stroke amplitude and frequency. The control of stroke kinematics, in turn, resides in the set of direct synchronous control muscles that insert on or near the sclerites of the wing hinge (Dickinson and Tu, 1997). Recently, Heide and Götz (1996) have identified at least some of the muscles responsible for the changes in wing kinematics underlying force control in *D. melanogaster*. Sustained activity in the large second basalar muscle (b2) is correlated with a pronounced increase in stroke amplitude (Lehmann, 1994; Heide and Götz, 1996). Even a single spike in b2 is sufficient to cause a transient increase in stroke amplitude (Lehmann and Götz, 1996). Another basalar muscle, b1, is tonically active in *D. melanogaster*, firing a single action potential in a narrow phase band within each wing stroke (Heide, 1983). Phase advances in the firing of b1 are correlated with increases in stroke amplitude in *D. melanogaster* (Heide and Götz, 1996), *Calliphora vicina* (Tu and Dickinson, 1996) and *Musca domestica* (Egelhaaf, 1989). In *Calliphora vicina*, these changes in firing phase appear to alter wing kinematics through their effect on muscle stiffness (Tu and Dickinson, 1994; Dickinson and Tu, 1997). In *D. melanogaster*, phase advances may similarly increase the biomechanical efficacy of b2 during its episodic firing (Lehmann and Götz, 1996). In contrast to b1 and b2, at least one muscle, I1, appears to function in decreasing the stroke amplitude of the wing (Heide and Götz, 1996). The activities of all three of these muscles (b1, b2 and I1) are modulated by visual pattern motion in a way that is consistent with the changes in stroke amplitude reported here (Heide and Götz, 1996).

The control of stroke frequency is thought to reside within the two pleurosternal muscles, ps1 and ps2, which are well placed to alter the resonance properties of the thorax (Boettiger and Furshpan, 1952; Boettiger, 1957). Electrophysiological recordings in blowflies (*Calliphora* spp.) do show a correlation between wingbeat frequency and the spike rate of the pleurosternal muscles (Nachtigall and Wilson, 1967; Heide, 1971; Kutsch and Hug, 1981). There are several other muscles whose activities might also result in a stiffening of the thoracic box, including the tergopleural muscles (tp1 and tp2) as well as the dorsal-longitudinal and dorsal-ventral asynchronous power muscles. In response to optomotor lift stimuli that elicit an increase in either lift or thrust, *D. melanogaster* modulates the spike frequency of both the left and right dorso-ventral power muscles by approximately 70 % (Heide *et al*. 1985). Although these asynchronous muscles are stretch-activated, power and stiffness must depend to some degree on the spike frequency of the neural input (Dickinson *et al*. 1997).

One of the most peculiar features of the flight-control system that we observed was the decrease in stroke frequency during the production of the highest flight forces, particularly prominent in *D. melanogaster* and *D. virilis* (Figs 3, 4). One explanation for this response is that stroke frequency at high flight forces is actively regulated by a decrease in the firing rate of frequency-controlling muscles (e.g. ps1 and ps2). An alternative explanation is that the decrease in stroke frequency results from a performance limit of the power muscles. It is possible that the firing rates of both the power muscles and the frequency-controlling muscles saturate at forces approximating body weight. In order to generate flight forces in excess of body weight, a fly uses steering muscles (e.g. b1 and b2) to increase stroke amplitude. Since they are already maximally activated, the power muscles might not be able to sustain a further increase in strain amplitude without a concomitant decrease in contraction frequency. It should be possible to test between these two alternatives by recording from control muscles while the flies are modulating force production.

The neuromuscular control of the mean force coefficient

Compared with the identification of the muscles responsible for changes in stroke amplitude and frequency, much less is known of the muscles controlling the more subtle aspects of stroke kinematics that might underlie changes in the mean force coefficient. In addition to their influence on amplitude, b1 and b2 also control finer aspects of stroke kinematics. In *Calliphora vicina*, phase advances in b1 and single b2 spikes cause the wing to follow a more anterior trajectory during the downstroke, changing the wing stroke from a figure-of-eight to an open ellipse (Tu and Dickinson, 1996). The aerodynamic consequences of this kinematic alteration are not well understood, but it is likely to result in increased force production since the changes occur in the wing stroke on the outside of an intended turn. In *D. melanogaster*, electrical stimulation of b2 decreases the rotational speed of the

ipsilateral wing by 50 % during the clap and fling, which might alter the efficacy of this important mechanism at the start of the downstroke (Lehmann, 1994). Advances in b1 phase (Heide, 1983; Heide and Götz, 1996) are correlated with advances in the timing of the ventral flip (Dickinson *et al*. 1993), which might influence the rotational mechanisms functioning during ventral stroke reversal. On the basis of morphology, the muscles of the third (III1–4) and fourth (hg1–4) axillary sclerites are thought to control wing supination and pronation and thus might regulate the angle of attack throughout the stroke (Pfau, 1977; Miyan and Ewing, 1985; Wisser, 1987, 1988). To date, however, there are no direct physiological or kinematic data to support these functions, and one muscle of the third sclerite (III1) is definitely not active during steering responses in *D. melanogaster* (Heide and Götz, 1996). Although we are only beginning to understand how the steering muscles control stroke kinematics, it is clear that the system is capable of many subtle alterations that could potentially influence the aerodynamic performance of the wings.

The magnitude of the mean force coefficient

The calculated values of the mean force coefficient, $\overline{C_F}$, when flight force is equal to body weight (Table 4) are significantly greater than those expected under steady-state conditions (*D. virilis*, 0.87, Vogel, 1967; *D. melanogaster*, 0.67, Zanker and Götz, 1990). Our definition of $\overline{C_F}$ includes the effects of several circulatory mechanisms, any or all of which might be responsible for the elevation of performance above that expected under steady-state conditions. Insect wings can generate circulation in three different ways: by translation, by rotation and by vortex capture (Ellington, 1984*d*). Recent flow-visualization studies using real and model hawkmoths suggest that an unsteady translational mechanism, delayed stall, is the primary means of force generation in large insects (Ellington *et al*. 1996; Willmott *et al*. 1996). The delayed stall is manifest as a transiently stable attached vortex bubble on the leading edge of the wing during the downstroke. These studies did not detect a prominent leading-edge vortex during the upstroke, suggesting that this portion of the stroke is less important in force generation. In addition, they found no evidence for the capture of rotational vorticity at the start of the downstroke. Although the Reynolds number is much lower in *Drosophila* species than in hawkmoths, delayed stall during the downstroke is also likely to be the primary force-generating mechanism in these flies. In a two-dimensional model of a fruit fly, a prominent leading-edge vortex is generated at the angle of attack appropriate for the downstroke (Dickinson and Götz, 1993). Flow visualizations of tethered *D. melanogaster* support the formation of one tip vortex ring during the downstroke, with no comparable structure being generated during the upstroke (Dickinson and Götz, 1996). The absence of an upstroke vortex ring implies that the wing generates little or no translational vorticity during this portion of the stroke. This asymmetry in force generation might result from the asymmetry in kinematics, in that a clap and fling functions to develop circulation at the start of the downstroke but there is no comparable mechanism at the start of the upstroke. Furthermore, the development of vorticity during the upstroke on the isolated, non-clapping wings should be inhibited by the presence of the shed downstroke vorticity (Dickinson, 1996; Dickinson and Götz, 1996).

The observations outlined above suggest that our measurement of $\overline{C_F}$ represents, for the most part, an elevated translational force coefficient achieved by delayed stall during the downstroke. The values of $\overline{C_F}$ in *D. melanogaster*, derived at a flight force equal to body weight and calculated under the assumption that force production is limited to a downstroke representing 70 % of the stroke cycle, were 3.6 and 4.4 for the harmonic and sawtooth velocity models respectively (Table 4). In comparison, an impulsively started two-dimensional model *Drosophila* wing achieves a peak lift coefficient of 2.0 (Dickinson and Götz, 1993). This value is attained after two chord lengths of motion when the effect of delayed stall is greatest. In a hovering animal, the total pressure force generated by the wings (i.e. the resultant of lift *and* pressure drag) is potentially available as a source of weight support. For example, an insect might flap its wings in such a way that the surface of the wing was parallel to the ground throughout the downstroke. In this situation, delayed stall of a two-dimensional model wing produces a total peak force coefficient of 3.4 (Dickinson, 1996), which is still lower than the estimates of $\overline{C_F}$ derived from the present study. In addition, phase-reconstructed wing kinematics of tethered flies (Zanker, 1990; Zanker and Gotz, 1990) suggest that the orientation of the wing would not allow all the pressure force to be used in weight support during the downstroke. For this reason, the actual mean total force coefficient that the wings achieve is probably greater than our present estimates and is substantially larger than can be explained by delayed stall on a two-dimensional wing.

The discrepancy between the force coefficient values measured in the present study and those of the model wing have three possible explanations. First, it may be that published kinematic data are flawed, such that nearly all of the circulatory force during the downstroke is oriented perpendicular to the stroke plane. Second, it might be that the performance of three-dimensional wings is better than that of two-dimensional wings because of the stabilizing influence of axial flow (Ellington *et al*. 1996). This seems unlikely, since the $\overline{C_F}$ of 3.4 for a three-dimensional model represents the transient maximum for an unstable attached vortex. Axial flow might stabilize this performance over a longer translational distance (akin to the high-lift mechanism of the Concorde aeroplane), but it is not likely to elevate the circulation above the transient maximum of the two-dimensional case. The third explanation is that, in addition to delayed stall, other mechanisms play a roll in force generation. Laser interferometric measurements of instantaneous forces obtained in conjunction with flow visualization studies suggest that flies generate an upward force during the initial stages of the upstroke (Dickinson and Götz, 1996), just after the occurrence of the ventral flip (Dickinson

et al. 1993). This would suggest, contrary to the evidence given above, that upstroke translation and/or a rotational mechanism contribute to the total upward force. Indeed, if pressure force does have a rearward component during the downstroke, then the wings must at some point generate a balancing forward force if the animal is to hover. The current paradox is that, while this predicted force generation should leave an imprint in the wake in the form of shed tip vorticity as required by Helmholtz laws, such structures have not been visualized (Dickinson and Götz, 1996). Since the resolution of flow visualizations in *Drosophila* spp. is unlikely to improve in the near future, the best opportunity for resolution of this discrepancy is probably with the use of accurate three-dimensional wing models (Ellington *et al*. 1996).

Force coefficients and body size

The gross effects of body size on force production can be assessed by considering a simple aerodynamic model:

$$F_t \propto \overline{C_F}(R\Phi n)^2 S \ . \quad (7)$$

For an isometric group of animals, wing length, R, is proportional to any linear dimension (L), surface area (S) is proportional to L^2 and body weight to L^3. The above relationship therefore reduces to:

$$L^3 \propto \overline{C_F}\Phi n L^4 \ . \quad (8)$$

In order for an animal to support its body weight at all sizes, the product $\overline{C_F}\Phi n$ must scale with L^{-1}. Of the two kinematic variables measured in the present study, stroke frequency decreased with body size among the four drosophilid species, while stroke amplitude did not (Fig. 9A,B). However, the increased stroke frequency of small flies did not completely compensate for the reduction in translational velocity. Consequently, the $\overline{C_F}$ required in the smallest species, *D. nikananu*, is nearly 1.5 times that needed by the larger species (Fig. 9E; Tables 3, 4). How does *D. nikananu* improve on the already remarkable aerodynamic performance attained by the larger drosophilids? One possibility is that these small flies utilize a strong clap and fling to initiate an especially robust leading-edge vortex. To test the feasibility of this hypothesis, we recorded short flight sequences on video tape and measured the dorsal excursion of the wings within the stroke cycle. The results suggest that the wing stroke is similar among all species, with the exception of *D. mimica*, which exhibited a 'near' clap in which the tips of the wings remain approximately parallel and do not touch during stroke reversal. We cannot exclude the possibility that *D. nikananu* might rotate its wings more quickly during the clap and fling or vary its kinematics in a way that is not easily seen with our simple video analysis. Another possibility is that *D. nikananu* might increase its aerodynamic performance by using a higher angle of attack during the downstroke. In accordance with the ambiguities discussed above, *D. nikananu* might also achieve higher force coefficient values by augmenting rotational mechanisms during the ventral flip or by increasing upstroke lift. Unfortunately, there are few data to help distinguish among these possible explanations for the extraordinary performance of *D. nikananu*.

Whatever the active mechanisms that produce the augmented lift in *D. nikananu*, it is not clear why the larger species do not increase their aerodynamic performance by the same means. These larger species could attain the same flight forces at lower stroke frequency and amplitude (and thereby lower cost) which would be beneficial if selection acted to optimize energy efficiency. It may be that the design of the flight system represents a compromise between energy efficiency and maneuverability. While the small flies must operate at near their maximum levels of performance just to stay in the air, larger flies might possess a greater performance reserve that they could utilize in the production of more elaborate flight behaviors. This explanation is not supported by comparing the maximum flight performance of the four species in the present study. The mean maximum hovering flight force for *D. nikananu* was 140 % of body weight, while the values for two larger species, *D. melanogaster* and *D. mimica*, were 134 % and 87 %, respectively (Table 3). Such comparisons must be viewed cautiously, however, since such differences may be related to the phylogenetic history of the species and not to body size *per se*. An alternative explanation for the elevated force coefficients in *D. nikananu* is that, while the kinematic patterns are similar among the four species, aerodynamic performance is actually *enhanced* at lower Reynolds number (Fig. 10). Although fluid viscosity attenuates vorticity, it may also act to stabilize vortex shedding. Such stabilization is well illustrated by the reduction in the shedding frequency of a von Karman street (the Strouhal number) with decreasing Reynolds number (Schlichting, 1979), and might act to prolong delayed stall during the downstroke. If this hypothesis proves true, then there exists a small window of intermediate Reynolds numbers ($50<Re<100$) in which the increased viscous dissipation is great enough to stabilize an attached vortex, but small enough so as not to attenuate its strength prohibitively.

List of symbols

$\bar{c}$	mean chord length of the wing
$\hat{c}$	dimensionless chord length
$\overline{C_F}$	mean force coefficient of the wing
$c(r)$	chord length of wing section
F_t	average total flight force generated by wing pair during stroke
L	linear dimension of body
n	stroke frequency
r	distance from wing base to wing section
$\hat{r}$	dimensionless distance from base to wing section
$\hat{r}_2^2(S)$	normalized second moment of wing area
R	wing length
Re	Reynolds number

S	surface area of wing
$\hat{t}_f$	dimensionless stroke time contributing to weight support
$\overline{u}(r)$	mean translational velocity of wing section
$\overline{u_r}(r)$	mean relative velocity of wing section
$\overline{u^2}(r)$	mean square translational velocity of wing section
$\overline{u_r^2}(r)$	mean square relative wing velocity of wing section
$\overline{u_r}(S)$	mean relative velocity of wing center of area
$\overline{u_r^2}(S)$	mean square relative velocity of wing center of area
$\overline{u_r}(R)$	mean relative velocity of wing tip
w_b	body weight
β	angle of stroke plane
β_r	angle of relative stroke plane
Φ	stroke amplitude
$\mathrm{d}\hat{\phi}/\mathrm{d}\hat{t}$	dimensionless wing velocity
$\overline{\lvert \mathrm{d}\hat{\phi}/\mathrm{d}\hat{t} \rvert^2}$	mean square of dimensionless wing velocity
$\overline{\Gamma}$	mean circulation generated by wing pair
ν	kinematic viscosity of fluid
ϕ	angular position of wing within stroke plane
ρ	density of air
ω_s	angular velocity of the background stripes

We would like to thank Jeff Hamlin for help with the morphological measurements required for this study. The project was funded by a Packard Foundation Fellowship and NSF grant IBN-9208765 (to M.H.D.) and a DFG Post-Doctoral Fellowship (to F.-O.L.).

References

BOETTIGER, E. G. (1957). The machinery of insect flight. In *Recent Advances in Invertebrate Physiology* (ed. B. T. Scheer), pp. 117–142. Eugene: University of Oregon Publications.

BOETTIGER, E. G. AND FURSHPAN, E. (1952). The mechanics of flight movements in Diptera. *Biol. Bull. mar. biol. Lab., Woods Hole* **102**, 200–211.

DAVID, C. T. (1978). The relationship between body angle and flight speed in free flying *Drosophila*. *Physiol. Ent.* **3**, 191–195.

DICKINSON, M. (1996). Unsteady mechanisms of force generation in aquatic and aerial locomotion. *Am. Zool.* **36**, 537–554.

DICKINSON, M. H. AND GÖTZ, K. G. (1993). Unsteady aerodynamic performance of model wings at low Reynolds numbers. *J. exp. Biol.* **174**, 45–64.

DICKINSON, M. H. AND GÖTZ, K. G. (1996). The wake dynamics and flight forces of the fruit fly *Drosophila melanogaster*. *J. exp. Biol.* **199**, 2085–2104.

DICKINSON, M. H., LEHMANN, F.-O. AND CHAN, W. P. (1997). The control of mechanical power in insect flight. *Am. Zool.* (in press).

DICKINSON, M. H., LEHMANN, F.-O. AND GÖTZ, K. G. (1993). The active control of wing rotation by *Drosophila*. *J. exp. Biol.* **182**, 173–189.

DICKINSON, M. H. AND TU, M. S. (1997). The function of dipteran flight muscle. *Comp. Biochem. Physiol.* A **116**, 223–238.

DUDLEY, R. AND ELLINGTON, C. (1990). Mechanics of forward flight in bumblebees. II. Quasi-steady lift and power requirements. *J. exp. Biol.* **148**, 53–88.

EGELHAAF, M. (1989). Visual afferences to flight steering muscles controlling optomotor responses of the fly. *J. comp. Physiol.* A **165**, 719–730.

ELLINGTON, C. P. (1984*a*). The aerodynamics of hovering insect flight. I. The quasi-steady analysis. *Phil. Trans. R. Soc. Lond. B* **305**, 1–15.

ELLINGTON, C. P. (1984*b*). The aerodynamics of insect flight. II. Morphological parameters. *Phil. Trans. R. Soc. Lond. B* **305**, 17–40.

ELLINGTON, C. P. (1984*c*). The aerodynamics of insect flight. III. Kinematics. *Phil. Trans. R. Soc. Lond. B* **305**, 41–78.

ELLINGTON, C. P. (1984*d*). The aerodynamics of insect flight. IV. Aerodynamic mechanisms. *Phil. Trans. R. Soc. Lond. B* **305**, 79–113.

ELLINGTON, C. P. (1984*e*). The aerodynamics of insect flight. VI. Lift and power requirements. *Phil. Trans. R. Soc. Lond. B* **305**, 145–181.

ELLINGTON, C. P. (1995). Unsteady aerodynamics of insect flight. In *Biological Fluid Dynamics*, vol. 49 (ed. C. P. Ellington and T. J. Pedley), pp. 109–129. London: Company of Biologists.

ELLINGTON, C. P., BERG, C. V. D., WILLMOTT, A. P. AND THOMAS, A. L. R. (1996). Leading-edge vortices in insect flight. *Nature* **384**, 626–630.

ENNOS, A. R. (1989). The kinematics and aerodynamics of the free flight of some Diptera. *J. exp. Biol.* **142**, 49–85.

GÖTZ, K. G. (1983). Bewegungssehen and Flugsteuerung bei der Fliege *Drosophila*. In *BIONA-Report 2* (ed. W. Nachtigall), pp. 21–34. Stuttgart: Fischer.

GÖTZ, K. G. (1987). Course-control, metabolism and wing interference during ultralong tethered flight in *Drosophila melanogaster*. *J. exp. Biol.* **128**, 35–46.

GÖTZ, K. G. AND WANDEL, U. (1984). Optomotor control of the force of flight in *Drosophila* and *Musca*. II. Covariance of lift and thrust in still air. *Biol. Cybernetics* **51**, 135–139.

GÖTZ, K. G. AND WEHRHAN, C. (1984). Optomotor control of the force of flight in *Drosophila* and *Musca*. I. Homology of wingbeat-inhibiting movement detectors. *Biol. Cybernetics* **51**, 129–134.

HEIDE, G. (1971). Die Funktion der nicht-fibrillären Flugmuskeln bei der Schmeißfliege *Calliphora*. II. Muskuläre Mechanismen der Flugssteuerung und ihre nervöse Kontrolle. *Zool. Jb. Physiol.* **76**, 99–137.

HEIDE, G. (1983). Neural mechanisms of flight control in Diptera. In *BIONA-Report 2* (ed. W. Nachtigall), pp. 35–52. Stuttgart: Fischer.

HEIDE, G. AND GÖTZ, K. G. (1996). Optomotor control of course and altitude in *Drosophila* is achieved by at least three pairs of flight steering muscles. *J. exp. Biol.* **199**, 1711–1726.

HEIDE, G., SPÜLER, M., GÖTZ, K. G. AND KAMPER, K. (1985). Neural control of asynchronous flight muscles in flies during induced flight manoeuvers. In *Insect Locomotion* (ed. G. Wendler), pp. 215–222. Berlin: Paul Parey.

HEISENBERG, M. AND WOLF, R. (1979). On the fine structure of yaw torque in visual flight orientation of *Drosophila melanogaster*. *J. comp. Physiol.* A **130**, 113–130.

HEISENBERG, M. AND WOLF, R. (1984). *Vision in* Drosophila. Berlin: Springer-Verlag.

HEISENBERG, M. AND WOLF, R. (1988). Reafferent control of optomotor yaw torque in *Drosophila melanogaster*. *J. comp. Physiol.* A **163**, 373–388.

KUTSCH, W. AND HUG, W. (1981). Dipteran flight motor pattern: Invariabilities and changes during postlarval development. *J. Neurobiol*. **12**, 1–14.

LEHMANN, F.-O. (1994). Aerodynamische, kinematische und electrophysiologische Aspekte der Flugkrafterzeugung und Flugkraftsteuerung bei der Taufliege *Drosophila melanogaster*. Thesis, Eberhad-Karls-Universität Tübingen.

LEHMANN, F.-O. AND DICKINSON, M. H. (1997). The changes in power requirements and muscle efficiency during elevated force production in the fruit fly *Drosophila melanogaster*. *J. exp. Biol*. **200**, 1133–1143.

LEHMANN, F.-O. AND GÖTZ, K. G. (1996). Activation phase ensures kinematic efficacy in flight-steering muscles of *Drosophila melanogaster*. *J. comp. Physiol*. **179**, 311–322.

MAXWORTHY, T. (1979). Experiments on the Weis-Fogh mechanism of lift generation by insects in hovering flight. 1. Dynamics of the 'fling'. *J. Fluid Mech*. **93**, 47–63.

MIYAN, J. A. AND EWING, A. W. (1985). How Diptera move their wings: a re-examination of the wing base articulation and muscle systems concerned with flight. *Phil. Trans. R. Soc. Lond. B* **311**, 271–302.

NACHTIGALL, W. (1966). Die Kinematik der Schlagflügelbewegungen von Dipteren. Methodische und Analytische Grundlagen zur Biophysik des Insektenflugs. *Z. vergl. Physiol*. **52**, 155–211.

NACHTIGALL, W. (1979). Rasche Richtungsänderungen und Torsionen schwingender Fliegenflügel und Hypothesen über zugeordnete instationäre Strömungseffekte. *J. comp. Physiol*. A **133**, 351–355.

NACHTIGALL, W. (1985). *Calliphora* as a model system for analyzing insect flight. In *Nervous System: Structure and Motor Function*, vol. 5 (ed. G. A. Kerkut and L. J. Gilbert), pp. 571–605. London: Pergamon Press.

NACHTIGALL, W. AND WILSON, D. M. (1967). Neuromuscular control of dipteran flight. *J. exp. Biol*. **47**, 77–97.

PFAU, H. K. (1977). Funktion einiger direkter tonischer Flügelmuskeln von *Calliphora erythrocephala* Miegen. *Verh. dt. zool. Ges*. **70**, 275.

RUDOLPH, R. (1976). Some aspects of wing kinematics in *Calopteryx splendens* (Harris) (Zygoptera: Calopterygidae). *Odonatologica* **5**, 59–64.

SCHLICHTING, H. (1979). *Boundary-Layer Theory*. New York: McGraw-Hill. 817pp.

TRIMARCHI, J. R. AND SCHNEIDERMAN, A. E. (1995*a*). Different neural pathways coordinate *Drosophila* flight initiations evoked by visual and olfactory stimuli. *J. exp. Biol*. **198**, 1099–1104.

TRIMARCHI, J. R. AND SCHNEIDERMAN, A. M. (1995*b*). Flight initiations in *Drosophila melanogaster* are mediated by several distinct motor patterns. *J. comp. Physiol*. A **176**, 355–364.

TU, M. S. AND DICKINSON, M. H. (1994). Modulation of negative work output from a steering muscle of the blowfly *Calliphora vicina*. *J. exp. Biol*. **192**, 207–224.

TU, M. S. AND DICKINSON, M. H. (1996). The control of wing kinematics by two steering muscles of the blowfly, *Calliphora vicina*. *J. comp. Physiol*. A **178**, 813–830.

VOGEL, S. (1967). Flight in *Drosophila*. III. Aerodynamic characteristics of fly wings and wing models. *J. exp. Biol*. **46**, 431–443.

VOGEL, S. (1981). *Life in Moving Fluids*. Princeton: Princeton University Press.

WAKELING, J. M. AND ELLINGTON, C. P. (1997). Dragonfly flight. II. Velocities, accelerations and kinematics of flapping flight. *J. exp. Biol*. **200**, 557–582.

WEIS-FOGH, T. (1973). Quick estimates of flight fitness in hovering animals, including novel mechanisms for lift production. *J. exp. Biol*. **59**, 169–230.

WILLMOTT, A. P., ELLINGTON, C. P. AND THOMAS, A. L. R. (1996). Flow visualization and unsteady aerodynamics in the flight of the hawkmoth *Manduca sexta*. *Phil. Trans. R. Soc. Lond. B* **352**, 303–316.

WISSER, A. (1987). Mechanisms of wing rotating regulation in *Calliphora erythrocephala* (Insecta, Diptera). *Zoomorph*. **106**, 261–268.

WISSER, A. (1988). Wing beat of *Calliphora erythrocephala*: turning axis and gearbox of the wing base (Insecta, Diptera). *Zoomorph*. **107**, 359–369.

ZANKER, J. M. (1990). The wing beat of *Drosophila melanogaster*. I. Kinematics. *Phil. Trans. R. Soc. Lond. B* **327**, 1–18.

ZANKER, J. M. AND GÖTZ, K. G. (1990). The wing beat of *Drosophila melanogaster*. II. Dynamics. *Phil. Trans. R. Soc. Lond. B* **327**, 19–44.